Materials Research. 2019; 22(suppl. 1): e20180852
DOI: https://doi.org/10.1590/1980-5373-MR-2018-0852

Thermomechanical Characterization of Superelastic Ni-Ti SMA Helical Extension Springs Manufactured by Investment Casting

José Joelson de Melo Santiago [a]****, Jackson de Brito Simões*** [b]***, Carlos José de Araújo*** [c]

[a]*Universidade Federal da Paraíba (UFPB), João Pessoa, PB, Brasil*
[b]*Universidade Federal Rural do Semi-Árido (UFERSA), Caraúbas, RN, Brasil*
[c]*Universidade Federal de Campina Grande (UFCG), Campina Grande, PB, Brasil*

Received: December 11, 2018; Revised: January 22, 2020; Accepted: March 10, 2020

Shape memory alloy (SMA) helical springs are special mechanical parts that require a previous evaluation of its behavior for application. Therefore, in this paper thermal and mechanical behaviour of superelastic Ni-Ti SMA helical extension springs manufactured by investment casting (IC) are evaluated. Phase transformation temperatures were measured by Electrical Resistance as a function of Temperature (ERT) and Differential Scanning Calorimetry (DSC). Tensile tests were carried out within strain and temperatures ranges. The pitch angle and stiffness of each spring were determined. Results demonstrated that Ni-Ti SMA helical springs produced by IC presented phase transformation corresponding to the superelastic effect (SE). The reversible deformations under tensile test were of the order of 70%. The mechanical behavior as function of temperature revealed a linear relationship between maximum force and spring temperature.

Keywords: *Shape Memory Alloy, Ni-Ti alloys, Helical Extension Springs, Investment Casting.*

1. Introduction

Since the discovery of the shape memory phenomenon in Ni-Ti alloys, shape memory alloys (SMA) have been applied in several areas such as aeronautics and biomedical. Ni-Ti SMA have excellent functional properties, biocompatibility and corrosion resistance. However, the high manufacturing costs due to high reactivity of Ti is a main drawback to the advancement of commercial applications[1-3].

In general, the manufacture of Ni-Ti alloys is accomplished through two main techniques, casting processes and powder metallurgy, followed by other processes such as machining, heat treatments, forming and shape setting to obtain mechanical devices[3,4]. Recently, additive manufacturing (AM) processes have also been used to produce Ni-Ti parts[3,5].

In order to establish an alternative route for the manufacture of Ni-Ti SMA parts, Simões and De Araújo[6] have recently used investment casting (IC) processes to produce various mechanical components such as Belleville washers, wire netting, honeycombs, helical springs and screws. Basically, in their work the Ni-Ti bulk material was obtained previously by a Plasma Skull Push Pull (PSPP) process, validated by De Araújo et al[7], and submitted to induction melting followed by centrifugal injection in ceramic moulds.

Among the mechanical Ni-Ti SMA parts, helical springs stand out. These mechanical components can be used as actuators and sensors. Amerinatanzi et al[8] evaluated the performance of a Ni-Ti superelastic spring and compared it with a stainless-steel spring applied to an ankle foot orthosis (AFO) hinged ankle support. In odontology, Ni-Ti springs are generally used for tooth movement because of their ability to provide constant forces[9]. Also, in recent decades, studies have shown the effectiveness of using SMA springs for seismic isolation [10]. Due to intrinsic shape memory effect, SMA springs can also be used as thermal actuators in valves[11]. More recently, SMA coil springs have been proposed for use as mechanical vibration attenuators in rotary systems[12,13].

Ni-Ti SMA springs are manufactured by "shape setting", wherein the wire is wrapped and fixed around a cylinder and then heat treated to obtain the coil spring shape. However, while usual and simple, this process depends on the preliminary fabrication of the Ni-Ti wires[4,14,15]. Thus, it is also important to develop processes for obtaining these components in a single manufacturing step, especially for custom applications. Recently, helical springs produced by investment casting techniques were obtained directly from the molten Ni-Ti and presented good mechanical properties[6,16].

However, there are not many studies on the thermomechanical behaviour of Ni-Ti alloy products obtained by investment casting. Thus, the international literature still needs to be enriched with new results in this field of research.

Then, this paper analysed the thermal and mechanical behaviour of Ni-Ti SMA helical extension springs obtained by an investment casting process corresponding to induction melting followed centrifugal casting (ICC).

2. Experimental Procedures

Geometric parameters can affect the helical springs behavior when subjected to large displacements.[17] Four main geometric parameters are usually considered in the designing of SMA helical springs[17,18]: wire diameter (*d*), spring diameter (*D*), number of active coils (N_a) and pitch

*e-mail: joelson.santiago@hotmail.com

angle (α). Figure 1 shows a schematic drawing of a Ni-Ti SMA produced in this work.

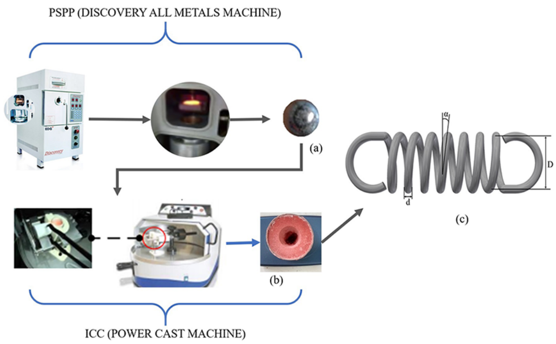

Figure 1. Flowchart of PSPP and ICC process of Ni-Ti SMA helical spring: (a) Ni-Ti SMA bulk, (b) Ceramic mould, (c) Ni-Ti SMA extension spring.

The main design parameter is known as spring index, which is the ratio $C = D/d$. Thus, it was selected the same spring index for all manufactured Ni-Ti SMA springs (C = 6), as summarized in Table 1.

Table 1. Spring geometric parameters.

Parameters / Springs	SPG-D1.0	SPG-D1.5	SPG-D2.0
Wire diameter (d, mm)	1.0	1.5	2.0
Spring diameter (D, mm)	6.0	9.0	12.0
Spring index (C)	6	6	6
Number of active coils (Na)	8	8	8
Pitch angle (α)	14.9º	10.1º	7.6º

SMA helical springs present a nonlinear distribution of shear stress due to phase transformations. However, in the initial linear region of the force (F) vs displacement (y) curve, with small variations in the pitch angle (α), the mechanical behaviour is similar to a conventional linear spring. Thus, it is possible to use a classic mathematical approach[19,20] to calculate the corresponding shear modulus (G) from stiffness (k) for SMA helical springs[18-21] in the austenitic phase using Eq. (1).

$$G = k\frac{8D^3N_a}{d^4} \tag{1}$$

Therefore, from force-displacement curves of superelastic SMA springs, as illustrated in Figure 2, stiffness (k) of the austenite phase is determined in the initial linear region from 10% to 20% of maximum load, before the transformation had taken place[21].

As previously mentioned, the manufacture process begins with the production of the Ni-Ti SMA material ($Ni_{50.2}Ti_{49.8}$, at. %) by a plasma melting process[7]. To manufacture the springs from the Ni-Ti SMA material, it was used an ICC

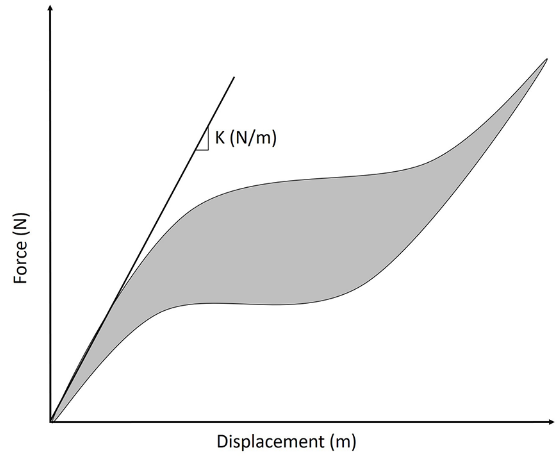

Figure 2. Schematic representation of the determination of stiffness (k) from a typical superelastic Force vs Displacement loop.

process. For this, ceramic moulds were produced from 3D printed wax springs[6].

After manufacturing, the Ni-Ti springs were submitted to heat treatment in a resistive furnace without protective atmosphere. The heat treatment applied was homogenization at 850ºC for 30min followed by ageing at 500ºC for 2h, both with air cooling[6].

The SMA characterization starts from the determination of phase transformation temperatures (PTTs). Critical transformation temperatures were measured by electrical resistance measured as a function of temperature (ERT) and differential scanning calorimetry (DSC). ERT is a non-destructive technique that allows analyse the average PTTs in the entire Ni-Ti coil spring. For this, SMA spring is placed into a thermal controlled silicone oil bath and submitted to a constant electrical current of low intensity to cause a potential difference between two points. Subsequently, the helical spring is subjected to cooling/heating between -60°C and 100°C with a 10°C min^{-1} rate using the thermal controlled bath (Hubber, CC 902 model). On the other hand, DSC is a technique that allows the measurement of the released and absorbed heat associated with the phase transformation in a small sample of the SMA spring. In this work it was used a heating/cooling rate of 10ºC min^{-1}, from -60°C to 100°C, using a DSC Q 20 model, from TA Instruments.

The as cast Ni-Ti springs were visually inspected with a digital microscope (Bluetek, model MC500), in order to analyse the surface quality and to identify superficial casting defects. Subsequently, the dimensions of the wax springs and manufactured springs were compared with a Profile Projector (Huatec Group, model HB16).

The heat-treated Ni-Ti SMA springs were mechanically characterized at room temperature (~25ºC) using a universal testing machine (Instron, 5582 model) equipped with a load cell of 30kN. A strain rate of 1% min^{-1} was used.

Initially, springs were loaded until failure to determine the maximum deflection for each spring. After that, quasi static tensile tests were carried out under three different maximum displacements of 50%, 60% and 70%. A strain rate of 1% min^{-1} was used during the loading and unloading. Subsequently, tensile tests at four different temperatures (30ºC, 40ºC, 50ºC and 60ºC) were performed only with the SPG-D2.0 spring (Tab. 1) under constant displacement (90%), due to its better mechanical behaviour in comparison with the other springs.

After the mechanical tests, a TESCAN Vega 3 Scanning Electron Microscopy (SEM) was used to examine the fractured surfaces of the Ni-Ti SMA springs.

3. Results and Discussion

3.1 Thermal characterization

Figure 3 shows the characteristic results obtained from ERT and DSC tests. For the thermal characterization, only the results for the spring SPG-D2.0 are presented, in both the as cast and heat-treated conditions. It was possible to confirm phase transformations in the Ni-Ti SMA springs in both conditions. A typical behaviour characteristic of the formation of the rhombohedral phase (R-phase) during cooling is observed, in both samples. There are many factors that can cause the R-phase formation in Ni-Ti SMA, such as heat treatment after cold work[22] and stress fields due to formation of Ni-rich precipitates [23].

Table 2 summarizes the TTs obtained from ERT and DSC curves (Figure 3). These two techniques yielded different transformation temperatures, which was mainly influenced by the sample state (as cast or HT) and sample dimensions (small sample for DSC and full spring for ERT). In addition, the Ni-Ti SMA materials are highly sensitive to thermomechanical processing and small composition variations[22]. Also, these two methods are based on different physical principles. DSC is a thermal analysis technique in which the heat flow of the material is measured as a function of temperature while ERT is based on changes in electric properties, usually applied to detect transformation temperatures between the martensite and austenite phases[24].

In general, after the heat treatment DSC peaks and ERT curves are more pronounced. According to De Araujo et al[25], internal stresses tend to increase the TTs of Ni-Ti SMA, which are reduced by the homogenization treatment. This behaviour was observed in heat treated springs, for which the A_f temperatures have been reduced.

3.2 Dimensional and superficial analysis

Figure 4 shows the Ni-Ti SMA extension springs manufactured by ICC. The springs present some defects such as burrs, bubbles and superficial roughness, typical of investment casting processes. The springs have matte grey surface, probably due to the reaction between the molten metal and ceramic mould, as pointed by Freitag et al[26].

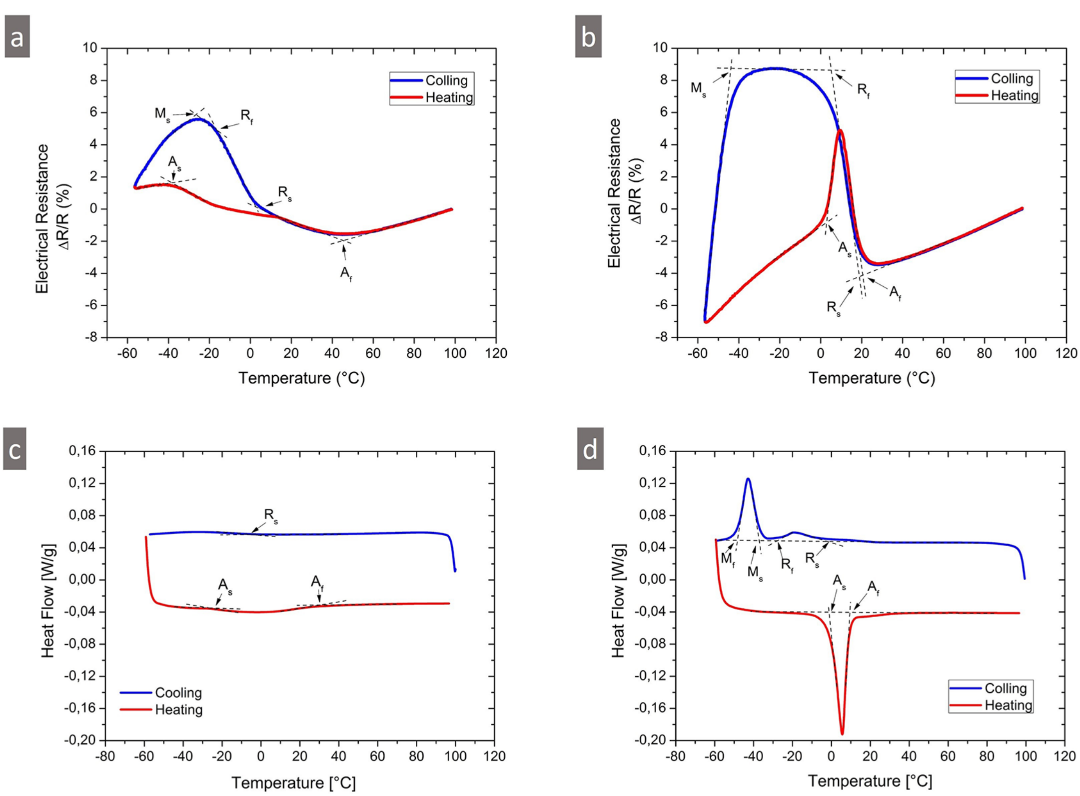

Figure 3. DSC and ERT behaviours for the SPG-D2.0 spring. a) ERT as-cast. b) ERT heat treated. c) DSC as-cast. d) DSC heat treated.

Table 2. Phase transformation temperatures of the as-cast and heat-treated Ni-Ti SMA springs by ERT and DSC techniques.

Springs ID	Test	State	Transformation temperatures (ºC)					
			M_f	M_s	R_f	R_s	A_s	A_f
SPG-D1.0	ERT	As Cast	-	-25.4	-	-	1.3	49.4
		HT	-30.3	-18.0	18.7	27.7	17.9	30.6
	DSC	As Cast	-	-11.5	-	-	-25.3	21.8
		HT	-48.5	-35.6	-27.8	-22.4	-3.7	11.7
SPG-D1.5	ERT	As Cast	-	-28.6	-13.8	1.11	-19.5	49.2
		HT	-54.9	-19.3	12.3	23.6	15.1	25.9
	DSC	As Cast				-5.4	-26.9	24.0
		HT	-53.8	-37.5	-33.2	-15.4	-4.7	9.6
SPG-D2.0	ERT	As Cast	-	-26.0	-16.4	2.2	-38.6	45.5
		HT	-	-43.6	5.3	18.9	3.2	21.0
	DSC	As Cast	-	-	-	-5.1	-26.4	28.7
		HT	-48.3	-36.6	-24.6	-6.3	-1.1	9.5

Figure 4. Some images of the Ni-Ti SMA springs manufactured by investment casting. a) SPG-D1.5. b) SPG-D1.0. c) SPG-D1.5. d) SPG-D2.0.

The dimensional accuracy was evaluated as the deviation of cast spring dimensions (wire diameter) from original wax model, as shown in Table 3. The maximum dimensional variation (contraction) was approximately 1.7%. Dimensional accuracy in titanium parts manufactured by investment casting is complex due the combination of thermal expansion effects of the coatings and metallic volumetric contraction[27].

An axial force applied to a helical springs produce a direct shear force and a torsional moment in the cross section[19,20]. Figure 5 shows a full view of the rupture surface

Table 3. Dimensional verification of the spring wire diameter (*d*).

Spring ID	Ni-Ti Spring	Wax Spring	Dimensional variation (%)
SPG-D1.0	1.10 ± 0.03	1.12 ± 0.08	1.7%
SPG-D1.5	1.51 ± 0.09	1.53 ± 0.09	1.3%
SPG-D2.0	2.07 ± 0.10	2.09 ± 0.10	1.2%

in SEM. Images present fractured surfaces characteristic of torsion, similar to those observed in orthodontic rotary instruments[28-30].

The presence of internal defects appears to be very important in the initiation of the fracture process of the springs. These defects act as points of stress concentration, leaving the spring more susceptible to failure. Notably, there were small voids distributed throughout the fractured surface. SEM analysis of the springs fractured by torsion revealed evidence of rupture along planes perpendicular at 45º to the longitudinal axis, typical behavior of brittle materials[31].

3.3 Tensile tests

Tensile tests were performed to analyse the mechanical behaviour of the cast Ni-Ti SMA helical springs. Each spring specimen was heated to a temperature above A_f and cooling below room temperature. Wire diameter is one of the four geometric parameters usually considered for

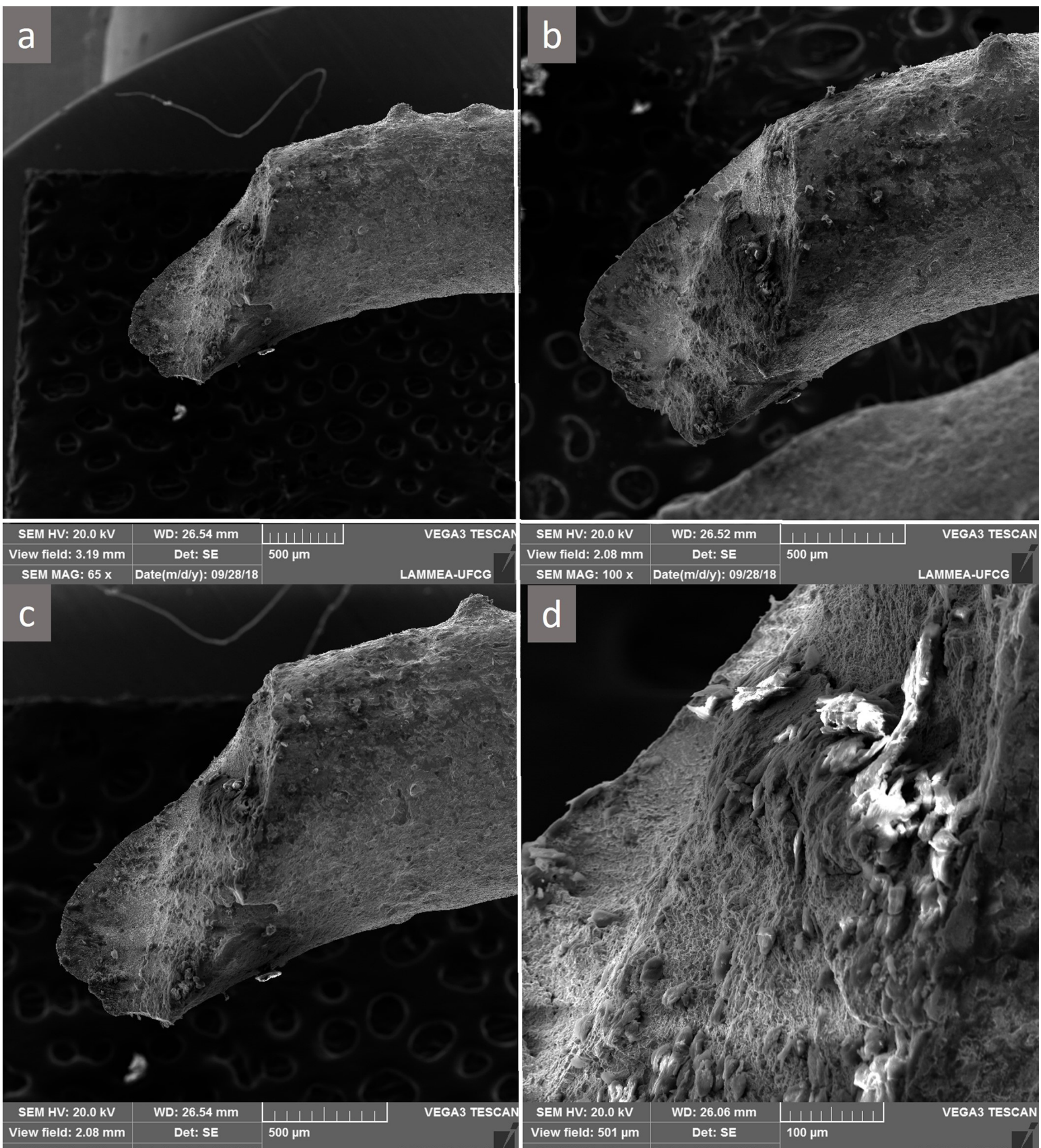

Figure 5. SEM of the SPG-D1.0 spring fractured surface after tensile tests. a) 65x. b) 100x. c) 100x. d) 415x.

the design of helical springs. Figure 6 shows the effect of variations of wire diameter on the force–displacement responses of the manufactured SMA springs. The increase of only 0.5 mm in the wire diameter can double the force values to produce the same deflection. The maximum force reached was 24N, 48N and 103N for the springs SPG-D1.0. SPG-D1.5 and SPG-D2.0, respectively, for 70% of maximum deflection.

According Shahinpoor and Schneider [32], there are three types of superelastic behavior in SMA work-hardened: superelasticity, linear superelasticity (when martensite is cold worked by about 10%), and nonlinear superelasticity (for which transformation occurs with strain at practically constant stress, presenting narrow hysteresis and small residual strain). Interestingly, the Ni-Ti SMA helical springs manufactured by ICC exhibit a quasi-linear superelasticity, recovering almost all the imposed strains, with narrow stress hysteresis, which is similar to the results of other previous studies[33,34]. Probably, this behavior results from the interaction between the nucleation of martensite in the Ni-Ti matrix phase (austenite) and residual stresses in precipitates during martensitic transformation[35,36].

3.4 Test temperature influence

Isothermal mechanical responses of the Ni-Ti SMA springs manufactured by ICC are shown in Figure 7 for tests at 30, 40, 50 and 60ºC. The springs change mechanical behaviour with temperature increase, showing a linear relationship between maximum force and test temperature. The force rate obtained from maximum force vs temperature linear relationship was of the order of 1.6 N/ºC.

From Figure 7, two considerable features are observed. First, the start point corresponding to the stress-induced martensite region increases with temperature. Full superelasticity was observed under tensile strain only at room temperature (30ºC), but not at 40ºC, 50ºC and 60ºC, due to the presence of higher levels of residual strain (10%). The increase of stress levels caused by the increase of applied forces at temperatures higher than 30ºC might have caused higher residual strains, due to possible plastic deformation of the material. Further, during transformation, the deformation is highly non-homogeneous, which might result in some voids of SMA which were not transformed from austenite into stress-induced martensite or vice-versa. These conclusions

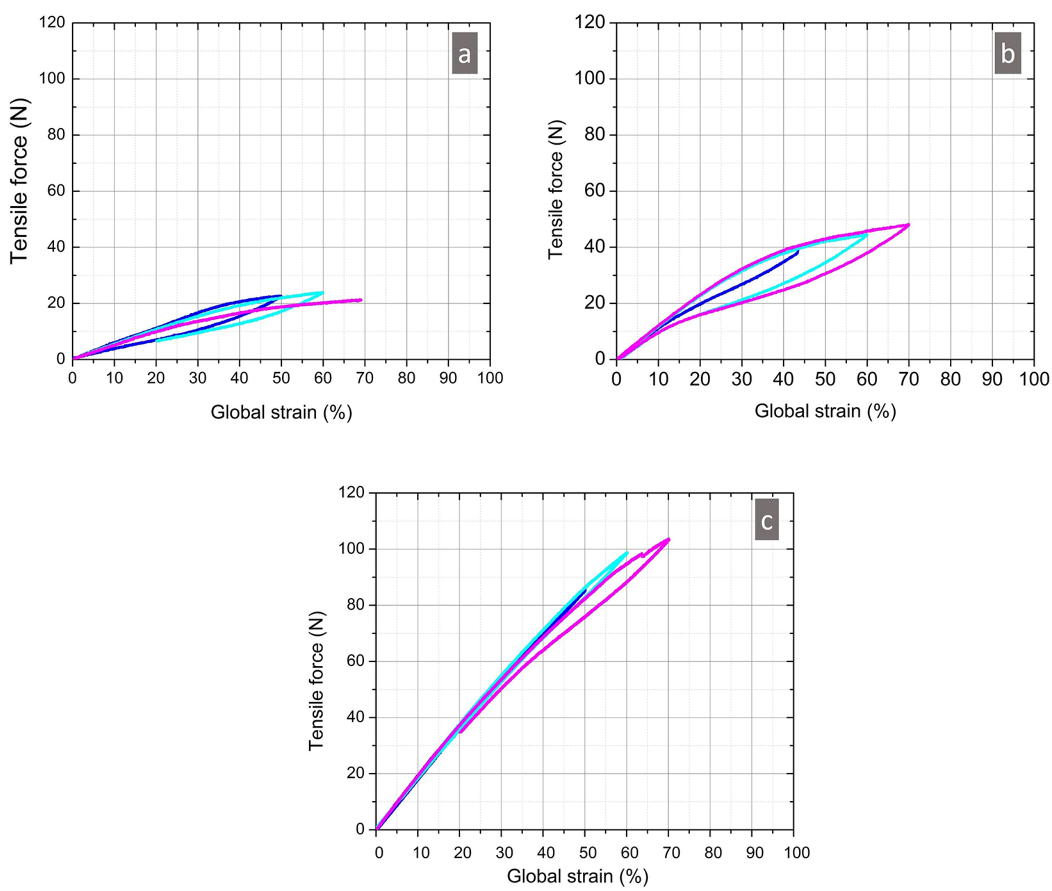

Figure 6. Force versus global strain for heat-treated Ni-Ti SMA springs. a) SPG-D1.0. b) SPG-D1.5. c) SPG-D2.0.

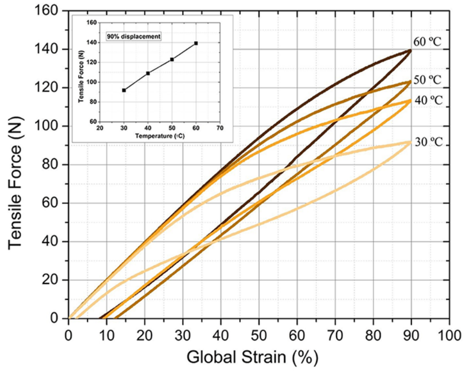

Figure 7. Force vs deflection behaviour for SPG-D2.0 as a function of temperature.

were based on previous characterization studies of shape memory alloys[37].

3.5 Stiffness (k) and shear modulus (G)

Although the SMA springs have nonlinear characteristics, it is possible to use the austenite stiffness to define mechanical aspects of the spring. Table 4 presents the measured stiffness (as defined in Fig. 2) and estimated shear modulus (Eq. 1) for the heat-treated Ni-Ti SMA springs. The obtained values are in the range found in the literature (25 ~ 40GPa) for Ni-Ti SMA in austenitic phase[17,18].

Table 4. Measured stiffness and calculated shear modulus of the Ni-Ti SMA superelastic helical springs.

Spring ID	Austenite Stiffness *k* (kN/m)	Shear Modulus *G* (GPa)
SPG-D1.0	2.2	25.5
SPG-D1.5	3.9	35.0
SPG-D2.0	5.6	31.2

4. Conclusions

This paper investigated the thermomechanical characterization of Ni-Ti shape memory alloy helical springs manufactured by centrifugal investment casting. The main conclusions that can be outlined from the obtained results are:

Ni-Ti SMA helical extension springs were successfully manufactured using investment casting. It was found that transformation temperatures decreased after heat treatment, in relation to as cast springs. In general, the reverse transformation temperatures ranging from -38.6 °C to 49.4 °C for as cast springs and -4.7ºC to 30.6ºC for heat treated springs.

At room temperature, the Ni-Ti SMA springs manufactured by investment casting exhibit a quasi-linear superelasticity behaviour (without force plateau) with residual strain around 1%. The maximum displacement supported without rupture were 70% for SPG-D1.0, SPG-D1.5, SPG-D2.0. The wire diameter affects significantly mechanical behaviour of the springs and an increase of only 0.5 mm in the wire diameter can double the force values to produce the same deformation.

The estimated austenitic shear modulus of the Ni-Ti SMA was between 25 and 35GPa, in agreement with literature (25 - 40GPa). The maximum force in the Ni-Ti SMA springs (2 mm of wire diameter) increases linearly with temperature, with a force rate of the order of 1,6 N/ºC.

5. Acknowledgments

The authors would like to thank UFERSA/UFCG by the technical cooperation accord N° 07/2017 23091.005950/2017-19 (project UFERSA PEG00001-2017, PIG00029-2017 and PIG20001-2020), as well as the CNPq Brazilian research agency for funding the following projects: National Institute of Science and Technology - Smart Structures in Engineering (Grant 574001/2008-5), Universal 01/2016 (Grant 401128/2016-4) and PQ-1C (Grant 302740/2018-0).

References

1. Lagoudas DC. *Shape memory alloys: modeling and engineering applications.* New York: Springer Publishing; 2008.

2. Jani JM, Leary M, Subic A, Gibson M. A review of shape memory alloy research, applications and opportunities. *Materials and Design*. 2014;56:1078-1113.

3. Elahinia MH. *Shape memory alloy actuators: design, fabrication and experimental evaluation*. New Jersey: Wiley; 2016.

4. Yamauchi K, Ohkata I, Tsuchiya K, Miyazaki S. *Shape memory and superelastic alloys: applications and technologies*. Cambridge: Woodhead Publishing; 2011.

5. Elahinia M, Moghaddam NS, Andani MT, Amerinatanzi A, Bimber BA, Hamilton RF. Fabrication of NiTi through additive manufacturing: a review. *Progress in Materials Science*. 2016;83:630-663.

6. Simões JB, Araújo CJ. Nickel–titanium shape memory alloy mechanical components produced by investment casting. *Journal of Intelligent Material Systems and Structure*. 2018;29(19):1045389X1879919.

7. Araújo CJ, Gomes AAC, Silva JA, Cavalcanti AJT, Reis RPB, Gonzalez CH. Fabrication of shape memory alloy using the plasma skull push-pull process. *Journal of Materials Processing Technology*. 2009;209(7):3657-3664.

8. Amerinatanzi A, Zamanian H, Moghaddam NS, Jahadakbar A, Elahinia M. Application of the superelastic NiTi spring in Ankle Foot Orthosis (AFO) to create normal ankle joint behavior. *Bioengineering (Basel)*. 2017;4(4):95.

9. Khanna R, Tikku T, Sachan K, Maurya RP, Verma G, Ojhae V. Evaluation of canine retraction following periodontal distraction using NiTi coil spring and implants – a clinical study. *Journal of Oral Biology and Craniofacial Research*. 2014;4(3):192-199.

10. Speicher M, Hodgson DE, DesRoches R, Leon RT. Shape memory alloy tension/compression device for seismic retrofit of buildings. *Journal of Materials Engineering and Performance*. 2009;18(5-6):746-753.

11. Czechowicz A, Langbein S. *Shape memory alloy valves*. New York: Springer Publishing; 2015.

12. Holanda SA, Silva AA, Araújo CJ, Aquino AS. Study of the complex stiffness of a vibratory mechanical system with shape memory alloy coil spring actuator. *Shock and Vibration*. 2014;2014:162781.

13. Borges JM, Silva AA, Araújo CJ, Pimentel RL, Aquino AS, Senko R, et al. On the active control of a rotor-bearing system using shape memory alloy actuators: an experimental analysis. *Journal of the Brazilian Society of Mechanical Sciences and Engineering*. 2018;40(5):269.

14. Rao A, Srinivasa AR, Reddy JN. *Design of Shape Memory Alloy (SMA) actuators*. New York: Springer Publishing; 2015.

15. Heidari B, Kadkhodaei M, Barati M, Karimzadeh F. Fabrication and modelling of shape memory alloy springs. *Smart Materials and Structures*. 2016;25(12):125003.

16. Santiago JJM, Silva PCS, Araújo CJ, Simões JB. Mechanical behavior of Ni-Ti SMA helical springs manufactured by investment casting. *Research and Development in Material Science*. 2018;5(2):606-611.

17. An SM, Ryu J, Cho M, Cho KJ. Engineering design framework for a shape memory alloy coil spring actuator using a static two-state model. *Smart Materials and Structures*. 2012;21(5):055009.

18. Savi MA, Pacheco PMCL, Garcia MS, Aguiar RAA, Souza LFG, Hora RB. Nonlinear geometric influence on the mechanical behavior of shape memory alloy helical springs. *Smart Materials and Structures*. 2015;24(3):035012.

19. Juvinall RC, Marshek KM. *Fundamentals of machine component design*. 5ª ed. New Jersey: John Wiley & Sons; 2015.

20. Budynas RG, Nisbett JK. *Shigley's mechanical engineering design*. 10th ed. Manhattan: McGraw-Hill; 2015.

21. Grassi END, Oliveira HMR, Araujo CJ, Castro WB. Effect of heat treatments on the thermomechanical behaviour of Ni-Ti superelastic mini coil springs. *MATEC Web of Conferences*. 2015;33:1-6.

22. Otsuka K, Wayman CM. *Shape memory materials*. Cambridge: Cambridge University Press; 1998.

23. Miyazaki S, Igo Y, Otsuka K. Effect of thermal cycling on the transformation temperatures of Ti-Ni alloys. *Acta Metallurgica*. 1986;34(10):2045-2051.

24. Airoldi G, Lodi DA, Pozzi M. The electric resistance of shape memory alloys in the pseudoelastic regime. *Journal of Physique IV France*. 1997;7(C5):507-512.

25. Araújo CJ, Morin M, Guénin G. Estimation of internal stresses in shape memory wires during thermal cycling under constant load: a macromechanical approach. *Journal of Intelligent Material Systems and Structures*. 2000;11(7):516-524.

26. Freitag L, Schafföner S, Faßauer C, Aneziris CG. Functional coatings for titanium casting molds using the replica technique. *Journal of the European Ceramic Society*. 2018;38(13):4560-4567.

27. Leal MB, Paulino SM, Pagnano VO, Bezzon OL. Influence of investment type and sprue number on the casting accuracy of titanium crown margins. *The Journal of Prosthetic Dentistry*. 2006;95(1):42-49.

28. Parashos P, Messer HH. Rotary NiTi instrument fracture and its consequences. *Journal of Endodontics*. 2006;32(11):1031-1043.

29. Lopes HP, Gambarra-Soares T, Elias CN, Siqueira Junior JF, Inojosa IFJ, Lopes WSP, et al. Comparison of the mechanical properties of rotary instruments made of conventional nickel-titanium wire, M-wire, or nickel-titanium alloy in R-phase. *Journal of Endodontics*. 2013;39(4):516-520.

30. Lopes HP, Elias CN, Vedovello GA, Bueno CE, Mangelli M, Siqueira Junior JF. Torsional resistance of retreatment instruments. *Journal of Endodontics.* 2011;37(10):1442-1445.

31. Dowling NE. *Mechanical behavior of materials: engineering methods for deformation, fracture, and fatigue*. 4th ed. England: Pearson Education; 2012.

32. Shahinpoor M, Schneider HJ. *Intelligent materials.* Cambridge: Royal Society of Chemistry; 2008.

33. Halani PR, Kaya I, Shin YC, Karaca HE. Phase transformation characteristics and mechanical characterization of nitinol synthesized by laser direct deposition. *Materials Science and Engineering: A*. 2013;559:836-843.

34. Zhang X, Zong H, Cui L, Fan X, Ding X, Sun J. Origin of high strength, low modulus superelasticity in nanowire-shape memory alloy composites. *Scientific Reports*. 2017;7:46360.

35. Lu B, Cui X, Feng X, Dong M, Li Y, Cai Z, et al. Direct rapid prototyping of shape memory alloy with linear superelasticity via plasma arc deposition. *Vacuum*. 2018;157:65-68.

36. Hao S, Cui L, Jiang D, Han X, Ren Y, Jiang J, et al. A transforming metal nanocomposite with large elastic strain, low modulus, and high strength. *Science*. 2013;339(6124):1191-1194.

37. Churchill CB, Shaw JA, Iadicola MA. Tips and tricks for characterizing shape memory alloy wire: Part 2—Fundamental isothermal responses. *Experimental Techniques*. 2006;33(1):51-62.